

This is the author's peer reviewed, accepted manuscript. However, the online version of record will be different from this version once it has been copyedited and typeset.

PLEASE CITE THIS ARTICLE AS DOI: 10.1063/5.0149870

High mobility of intrinsic defects in α -Ga₂O₃

Alexander Azarov^{1,a}, Jihyeon Park², Daewoo Jeon², and Andrej Kuznetsov^{1,a}

¹*Department of Physics, Centre for Materials Science and Nanotechnology, University of Oslo, PO Box 1048 Blindern, N-0316 Oslo, Norway*

²*Korea Institute of Ceramic Engineering & Technology, Jinju 52851, South Korea*

Migration properties of the intrinsic defects were investigated in α -Ga₂O₃ by controllable introduction of the lattice disorder with ion irradiation and monitoring its evolution as a function of ion dose, flux, and temperature. Already the dose dependence acquired at room temperature suggested prominently high mobility of intrinsic defects in α -Ga₂O₃, since we observed two distinct disordered regions - near the surface and in the bulk - instead of a Gaussian shape following the ballistic defects production process. Moreover, the disorder accumulation has shown to be highly sensitive to the variation of the ion flux and temperature, known in literature as the dose-rate effect. Therefore, by monitoring the process as a function of the flux and temperature we observed such dose-rate effect in α -Ga₂O₃ with an activation energy of 0.33 ± 0.04 eV, which we attributed to the migration barrier of the intrinsic defects in the Ga sublattice, from where we collected the experimental data. By setting these results in the context of the theoretical data available in literature, we argued that this energy may be attributed to the migration activation of the Ga self-interstitials in α -Ga₂O₃.

Key words: gallium oxide, rhombohedral phase (α -Ga₂O₃), dose-rate effect, intrinsic defects,

^{a)} Authors to whom correspondence should be addressed: alexander.azarov@smn.uio.no, andrej.kuznetsov@fys.uio.no

This is the author's peer reviewed, accepted manuscript. However, the online version of record will be different from this version once it has been copyedited and typeset.

PLEASE CITE THIS ARTICLE AS DOI: 10.1063/1.50149870

Currently gallium oxide (Ga_2O_3) attracts massive research attention because of its properties promising for applications in power electronics and deep ultra-violet optoelectronics [1,2]. Among all known Ga_2O_3 polymorphs [3], the rhombohedral phase conventionally labeled as α - Ga_2O_3 exhibits the widest bandgap of ~ 5.3 eV [4], making it particularly interesting for these applications. Despite the steadily growing interest on α - Ga_2O_3 during the past years [5-9], there are practically no experimental data reported in literature on the intrinsic defects energetics, otherwise needed for predictive device processing. Moreover, there are no theoretical predictions for migration barriers of intrinsic defects in α - Ga_2O_3 available in literature, even though the data for monoclinic beta-phase (β - Ga_2O_3) may be used as a context for the interpretations [10-14].

In this work, we collected a set of experimental data allowed us to estimate the activation energy limiting the migration of intrinsic defects in α - Ga_2O_3 . Our approach was to monitor the radiation disorder evolution as a function of ion dose, flux, and temperature. For that matter, we used Rutherford Backscattering spectrometry in channeling mode (RBS/C) directly measuring the disorder levels in our samples. Previously this method was applied for investigations of the defect energetics in other semiconductors, e.g. in Si [15], GaAs [16], SiC [17], β - Ga_2O_3 [10] etc. The methodology is based on the interpretations of the residual disorder in crystalline materials in terms of the balance between generation of defects and their out-diffusion/annihilation. As shown previously [10,15-17], this balance may be understood by systematic variations of the ion flux and irradiation temperature, keeping the dose constant. Indeed, the ion flux determines the time intervals between neighboring collision cascades, while the defect migration rates between the cascades obviously depend on temperature. In literature, this concept is also known as a dose-rate effect [10,15-17]. Thus, in the present work, we observed such dose-rate effect in α - Ga_2O_3 with an activation energy of 0.33 ± 0.04 eV, which we attributed to the migration barrier

This is the author's peer reviewed, accepted manuscript. However, the online version of record will be different from this version once it has been copyedited and typeset.

PLEASE CITE THIS ARTICLE AS DOI: 10.1063/1.50149870

of the intrinsic defects in the Ga sublattice, from where we collected the experimental data. By setting these results in the context of the data available for β -Ga₂O₃ we argued that this energy gives an estimate of the migration activation for Ga self-interstitials in α -Ga₂O₃.

In this work we used $\sim 1\mu\text{m}$ thick α -Ga₂O₃ films grown on sapphire substrates. The films were fabricated by halide vapor phase epitaxy (see details of the synthesis elsewhere [18]). The samples were implanted with 400 keV ⁵⁸Ni⁺ ions in a wide range of ion fluxes ($9.3\times 10^{11} - 4.4\times 10^{12}$ at.cm⁻²s⁻¹) and irradiation temperatures (25-500 °C) keeping the same the value of ion dose at 5×10^{15} cm⁻². In addition, the control samples were implanted with 400 keV ⁵⁸Ni⁺ ions to the lower (1×10^{15} cm⁻²) and higher (1×10^{16} and 2×10^{16} cm⁻²) doses at room temperature keeping the ion flux constant. The implantations were performed maintaining 7° off-angle orientation from normal direction to minimize channeling. The ion doses used in the present study correspond to the displacement per atom (DPA) range of 2.6-53 in the maximum of the defect generation function. The DPA values are calculated using the SRIM [19] vacancy generation profiles for a given dose, normalized to an atomic density of α -Ga₂O₃ ($n_{at}=10.3\times 10^{22}$ at/cm³). The SRIM calculations were performed with 25 eV and 28 eV as the displacement energies for Ga and O atoms, respectively. After implantations all samples were measured by Rutherford backscattering spectrometry in channeling mode (RBS/C) using 1.6 MeV He⁺ ions incident along [010] direction and backscattered into a detector placed at 165° relative the incident beam direction. Conventionally, the RBS/C yield collected as a function of the channel number, can be directly correlated with the relative disorder as a function of depth. Ultimately, a fully disorder – amorphous – material is signified by the RBS/C yield reaching the random signal level [20]. Notably, as shown previously, Ni atoms are not chemically interacting with (Ga₂O₃) for the concentration range used in the present experiment [21].

This is the author's peer reviewed, accepted manuscript. However, the online version of record will be different from this version once it has been copyedited and typeset.

PLEASE CITE THIS ARTICLE AS DOI: 10.1063/1.50149870

A set of the RBS/C spectra in Fig.1 illustrates the result of the disorder accumulation in α -Ga₂O₃ as a function of dose for the implants performed at room temperature, keeping the ion flux constant. For comparison, using the same color code, we plot the DPA profiles corresponding to each dose, as calculated by SRIM. Thus, the direct comparison of the RBS/C and SRIM data in Fig.1, suggests prominently high mobility of the intrinsic defects in α -Ga₂O₃, since we observed two distinct disordered regions in the RBS/C spectra - near the surface and in the bulk - instead of a Gaussian shape, as predicted by SRIM following the ballistic defects production process (with maximum at $R_{pd} \approx 100$ nm marked by an arrow). More specifically, it is seen that already for the lowest ion dose (1×10^{15} cm⁻²) the RBS/C spectrum exhibits two distinct disorder peaks located at the sample surface and deeper in the bulk. Notably, the amplitude of the surface peak rapidly increases as a function of dose, reaching the random level for the highest dose used (2×10^{16} cm⁻²); i.e. indicating the formation of the surface amorphous layer. In its turn, the disorder in the bulk remains far from the amorphous level even though its amplitude increases too. To explain the two-peak trend, we included the inset in Fig. 1 schematically showing one individual collision cascade generated by impinging ion, with vacancies and self-interstitials depicted by the open and closed circles, respectively. Note that for simplicity the Ga and O-related defects are not separated in the inset. The double-arrow in the inset illustrates the recombination of the point defects within the collision cascade, most efficiently occurring at the depth of R_{pd} , while the single-arrows indicate out-diffusion of defects, evidently occurring most efficiently towards the surface.

Importantly, such disorder behavior is dramatically different from that occurring in the β -Ga₂O₃ polymorph where the single disorder peak is located in the maximum of the nuclear energy deposition, i.e. R_{pd} [10,22]. In contrast, the disorder profiles in Fig. 1

This is the author's peer reviewed, accepted manuscript. However, the online version of record will be different from this version once it has been copyedited and typeset.

PLEASE CITE THIS ARTICLE AS DOI: 10.1063/1.50149870

resemble the trends for the radiation disorder accumulation in GaN, where the surface amorphous layer and bulk disorder peak were also observed in ion irradiation experiments at room temperature too [23,24]. Similarly to our explanations above for Fig.1, the formation of the surface defect peak in GaN was previously attributed to the defect migration from the region where they are generated towards the surface with subsequent trapping at the amorphous/crystalline interface advancing from the surface [23,24]. Thus, for this similarity, the surface disorder peak in α -Ga₂O₃ should be sensitive to the ion flux/temperature since the defect migration/interaction rates depends on both parameters. For that matter, for the rest of the experiment, we fixed the dose (at 5×10^{15} cm⁻²) and investigated the variations of the disorder levels as a function of the flux and temperature; i.e. measuring the dose-rate effect in α -Ga₂O₃.

Figs. 2(a) and (b) show examples of the RBS/C spectra illustrating the roles of the irradiation temperature and ion flux on the disorder formation in α -Ga₂O₃, respectively. It is seen from Fig.2(a) that the increase in the irradiation temperature up to 100 °C has practically no effect on the disorder profile. However, already for 150 °C the height of surface peak decreases and it becomes close to that in the virgin (unirradiated) sample for the 300 °C implants. In its turn, Fig. 2(b) shows the RBS/C spectra of the samples implanted at 100°C with different ion fluxes and it is clearly seen that the ion flux also affects mainly the surface disorder peak which exhibits a distinct decrease with lowering ion flux. Notably, the bulk disorder peak is less sensitive to the irradiation variation in Fig.2, so that for the rest of the dose rate analysis we consider the surface peak only.

At this end, we conclude that the behavior of the surface disorder peak, upon the flux/temperature variations, supports the fact that this peak is formed due to the

This is the author's peer reviewed, accepted manuscript. However, the online version of record will be different from this version once it has been copyedited and typeset.

PLEASE CITE THIS ARTICLE AS DOI: 10.1063/1.50149870

migration and trapping of the defects originally generated deeper in the bulk. Thus, in order to determine the energetics of this process and draw a conclusion about the defects responsible for the formation of the surface peak, we summarize the dose-rate results in Fig. 3. Specifically, Fig. 3 shows the relative height of the surface disorder peak as a function of the irradiation temperatures for three different ion fluxes. It is seen that the curves exhibit sigmoidal behavior with irradiation temperature and the data shift to higher temperatures with increasing ion flux following the trend observed in other semiconductors [10,15-17]. Further, for each ion flux a critical transition temperature was determined as an inflection point of the fitting curves in Fig. 3. The Arrhenius plot for the ion flux vs critical transition temperature determined is shown in the inset in Fig. 3 and it is seen that the data follow a trend with an activation energy of $E_a = 0.33 \pm 0.04$ eV.

As explained in the introductory part and as discussed in literature [10,15-17], the activation energy of the dose-rate effect is a measure of the dominating migration barrier of the intrinsic defects limiting the process; i.e. 0.33 ± 0.04 eV for α -Ga₂O₃. Thus, the remaining question: migration of what specific intrinsic defect limits the process. The answer to the question is challenging since all kind of defects from both sublattices are generated in the collision cascades and literature data on defect energetics in Ga₂O₃ polymorphs are limited.

Most of the theoretical [11-13] and experimental [10,14] works on migration energies of point defects in Ga₂O₃ are related to β -polymorph and even here there is a large discrepancies in the results. For example, the migration barriers were theoretically calculated to be in the range of 0.5-2.3 and 1.2-4.0 eV for the gallium (V_{Ga}) and oxygen vacancies (V_O), respectively [11]. Even lower values were obtained by Blanco *et al.*

This is the author's peer reviewed, accepted manuscript. However, the online version of record will be different from this version once it has been copyedited and typeset.

PLEASE CITE THIS ARTICLE AS DOI: 10.1063/1.50149870

where the migration barriers were estimated to be as low as 0.1 and 0.5 eV for V_{Ga} and V_{O} , respectively [12]. Recently, Frodaron *et al.* [13] have obtained much higher values of migration barriers for Ga-related defects in $\beta\text{-Ga}_2\text{O}_3$, strongly depending on the defect charge state and the crystal orientation. Experimentally, in $\beta\text{-Ga}_2\text{O}_3$, V_{Ga} migration barriers were estimated from the electrical measurements as 1.2 eV [14] and from the dose-rate effect data as 0.8 eV [10]. Notably, in Ref. 10, the authors attributed 0.8 eV to the migration barrier of V_{Ga} based on the comparison with the theory data available in literature at the time. However, the theoretical data revisited by Frodaron *et al.* [13] suggest that the migration barrier for Ga interstitials also falls into the range obtained in the dose rate experiment for $\beta\text{-Ga}_2\text{O}_3$.

As it holds to $\alpha\text{-Ga}_2\text{O}_3$, there are no literature data on the migration barriers for intrinsic defects to make a direct comparison with 0.33 ± 0.04 eV, as determined in this work. However, it is reasonable to limit our consideration to Ga-related defects since we analyze only the Ga-sublattice in the RBS/C spectra. Further, such relatively low activation energy (0.33 ± 0.04 eV) is not surprising, accounting that already at room temperature the disorder accumulation is efficiently suppressed as compared with that predicted by SRIM, see Fig. 1. Thus, as prime candidates we may consider either Ga vacancies or Ga interstitials migration to limit the process. Taking into account the experimental data for $\beta\text{-Ga}_2\text{O}_3$ [10,14] and the most recent theoretical data [13], we think the activation energy determined in the present experiment fits best a hypothesis of Ga interstitials to act as a limiting migration step. Notably, the argument with Ga interstitials as dominant defects responsible for the formation of the surface disorder peak, perfectly correlates with the RBS/C results, even though other contributions from the rest of the defect reactions cannot be excluded.

This is the author's peer reviewed, accepted manuscript. However, the online version of record will be different from this version once it has been copyedited and typeset.

PLEASE CITE THIS ARTICLE AS DOI: 10.1063/5.0149870

Finally, it should be mentioned that the obtained E_a for α -Ga₂O₃ is lower as compared to that of other semiconductors. Indeed, the activation energy of the dose-rate effect was measured to be 1.3 eV for SiC [17] and 0.9 eV for both Si and GaAs [15,16]. However, there are no experimental dose-rate data for other radiation tolerant semiconductors, such as GaN and ZnO, despite that there were a few attempts to investigate the role of an ion flux on the disorder buildup in these materials [23,25].

In conclusion, we study radiation defect dynamics in α -Ga₂O₃ single crystals implanted by 400 keV Ni ions with varying such parameters as ion dose, irradiation temperature and ion flux. Results show that, in contrast to β -polymorph, intrinsic defects in α -Ga₂O₃ are highly mobile even at room temperature, so the disorder buildup accumulates in two distinct regions corresponding to the surface and the crystal bulk behind the primary defect generation area. Furthermore, a strong dependence of the defect formation on the ion flux (so-called “dose-rate effect”) was observed in the temperature range of 25-300 °C for the surface disorder peak. Arrhenius analysis revealed that the dominant process limiting defect migration at the used temperature range occurs with an activation energy of ~0.33 eV. This value is lower than that in β -Ga₂O₃ and can be attributed to the migration barrier of Ga interstitials.

This is the author's peer reviewed, accepted manuscript. However, the online version of record will be different from this version once it has been copyedited and typeset.

PLEASE CITE THIS ARTICLE AS DOI: 10.1063/5.0149870

ACKNOWLEDGMENTS

M-ERA.NET Program is acknowledged for financial support via GOFIB project (administrated by the Research Council of Norway project number 337627). The international collaboration was enabled through the INTPART and UTFORSK Programs at the Research Council of Norway and the Directorate for Higher Education and Skills in Norway (NEARTEMS project number 322382 and SPECTRINKO project number UTF-2021/10210). This work was also partly supported by the K-Sensor Development Program (No RS-2022-00154729) funded by the Ministry of Trade, Industry and Energy (MOTIE, Korea). The Research Council of Norway is also acknowledged for the support to the Norwegian Micro- and Nano-Fabrication Facility, NorFab, project number 295864.

AUTHOR DECLARATIONS

Conflict of interest

The authors have no conflicts to disclose.

DATA AVAILABILITY

The data that supports the findings of this study are available within the article.

This is the author's peer reviewed, accepted manuscript. However, the online version of record will be different from this version once it has been copyedited and typeset.

PLEASE CITE THIS ARTICLE AS DOI: 10.1063/5.0149870

1. S. J. Pearton, J. Yang, P. H. Cary, F. Ren, J. Kim, M. J. Tadjer, and M. A. Mastro, "A review of Ga₂O₃ materials, processing, and devices", *Appl. Phys. Rev.* **5**, 011301 (2018).
2. M. J. Tadjer, "Toward gallium oxide power electronics", *Science* **378**, 724 (2022).
3. H. Y. Playford, A. C. Hannon, E. R. Barney, and R. I. Walton, "Structures of uncharacterised polymorphs of gallium oxide from total neutron diffraction", *Chem.-A Eur. J.* **19**, 2803 (2013).
4. S. Fujita, M. Oda, K. Kaneko, and T. Hitora, "Evolution of corundum-structured III-oxide semiconductors: Growth, properties, and devices," *Jpn. J. Appl. Phys.* **55**, 1202A3 (2016).
5. M. Biswas and H. Nishinaka, "Thermodynamically metastable α -, ε - (or κ -), and γ -Ga₂O₃: From material growth to device applications", *APL Mater.* **10**, 060701 (2022).
6. J. Bae, D.-W. Jeon, J.-H. Park, and J. Kim, "High responsivity solar-blind metal-semiconductor-metal photodetector based on α -Ga₂O₃", *J. Vac. Sci. Technol. A* **39**, 033410 (2021).
7. T. Kobayashi, T. Gake, Y. Kumagai, F. Oba and Y. Matsushita, "Energetics and electronic structure of native point defects in α -Ga₂O₃", *Appl. Phys. Express* **12**, 091001 (2019).
8. Y. Pan, "First-principles investigation of the influence of point defect on the electronic and optical properties of α -Ga₂O₃", *Int. J. Energy Research* **46**, 13070 (2022).
9. A. Y. Polyakov, V.I. Nikolaev, I. N. Meshkov, K. Siemek, P. B. Lagov, E. B. Yakimov, A. I. Pechnikov, O. S. Orlov, A. A. Sidorin, S. I. Stepanov, I. V. Shchemerov, A. A. Vasilev, A. V. Chernykh, A. A. Losev, A. D. Miliachenko, I.

This is the author's peer reviewed, accepted manuscript. However, the online version of record will be different from this version once it has been copyedited and typeset.

PLEASE CITE THIS ARTICLE AS DOI: 10.1063/5.0149870

- A. Khrisanov, Yu. S. Pavlov, U. A. Kobets, and S. J. Pearton, "Point defect creation by proton and carbon irradiation of α -Ga₂O₃" J. Appl. Phys. **132**, 035701 (2022).
10. A. Azarov, V. Venkatachalapathy, E. V. Monakhov, and A. Yu. Kuznetsov, "Dominating migration barrier for intrinsic defects in gallium oxide: dose-rate effect measurements", Appl. Phys. Lett. **118**, 232101 (2021).
 11. A. Kyrtsov, M. Matsubara, and E. Bellotti, "Migration mechanisms and diffusion barriers of vacancies in Ga₂O₃", Phys Rev. B **95**, 245202 (2017).
 12. M. A. Blanco, M. B. Sahariah, H. Jiang, A. Costales, and R. Pandey, "Energetics and migration of point defects in Ga₂O₃", Phys. Rev. B **72**, 184103 (2005).
 13. Y. K. Frodason, J. B. Varley, K. M. H. Johansen, Lasse Vines, and C. G. Van de Walle, "Migration of Ga vacancies and interstitials in β -Ga₂O₃", Phys. Rev. B **107**, 024109 (2023).
 14. M. E. Ingebrigtsen, A. Yu. Kuznetsov, B. G. Svensson, G. Alfieri, A. Mihaila, U. Badstübner, A. Perron, L. Vines, and J. B. Varley, "Impact of proton irradiation on conductivity and deep level defects in β -Ga₂O₃", APL Mater. **7**, 022510 (2019).
 15. P. J. Schultz, C. Jagadish, M. C. Ridgway, R. G. Elliman, and J. S. Williams, "Crystalline-to-amorphous transition for Si-ion irradiation of Si(100)", Phys. Rev. B **44**, 9118 (1991).
 16. R. A. Brown and J. S. Williams, "The amorphization kinetics of GaAs irradiated with Si ions", J. Appl. Phys. **83**, 7533 (1998).
 17. A. Yu. Kuznetsov, J. Wong-Leung, A. Hallen, C. Jagadish, and B. G. Svensson, "Dynamic annealing in ion implanted SiC: Flux versus temperature dependence", J. Appl. Phys. **94**, 7112 (2003).

This is the author's peer reviewed, accepted manuscript. However, the online version of record will be different from this version once it has been copyedited and typeset.

PLEASE CITE THIS ARTICLE AS DOI: 10.1063/5.0149870

18. H. Son and D.-W. Jeon, "Optimization of the growth temperature of α -Ga₂O₃ epilayers grown by halide vapor phase epitaxy", *J. Alloys and Comp.* **773**, 631 (2019).
19. J. F. Ziegler, M. D. Ziegler, and J. P. Biersack, "SRIM—the stopping and range of ions in matter (2010)", *Nucl. Instrum. Methods Phys. Res. B* **268**, 1818 (2010).
20. L. C. Feldman, J. W. Mayer, and S. T. Picraux, "Materials analysis by ion channeling", Academic Press 1982.
21. A. Azarov, C. Baziotti, V. Venkatachalapathy, P. Vajeeston, E. Monakhov, and A. Kuznetsov, "Disorder-induced ordering in gallium oxide polymorphs", *Phys. Rev. Lett.* **128**, 015704 (2022).
22. E. Wendler, E. Treiber, J. Baldauf, S. Wolf, and C. Ronning, "High-level damage saturation below amorphisation in ion implanted β -Ga₂O₃", *Nucl. Instrum. Methods Phys. Res. B* **379**, 85 (2016).
23. S. O. Kucheyev, J. S. Williams, C. Jagadish, J. Zou, and G. Li, "Damage buildup in GaN under ion bombardment", *Phys. Rev. B* **62**, 7510 (2000).
24. A. Yu. Azarov, A. I. Titov, and S. O. Kucheyev, "Effect of pre-existing disorder on surface amorphization in GaN", *J. Appl. Phys.* **108**, 033505 (2010).
25. A. Yu. Azarov, A. I. Titov, P. A. Karaseov, S. O. Kucheyev, A. Hallén, A. Yu. Kuznetsov, B. G. Svensson, A. P. Pathak, "Structural damage in ZnO bombarded by heavy ions", *Vacuum* **84**, 1058 (2010).

This is the author's peer reviewed, accepted manuscript. However, the online version of record will be different from this version once it has been copyedited and typeset.

PLEASE CITE THIS ARTICLE AS DOI: 10.1063/1.50149870

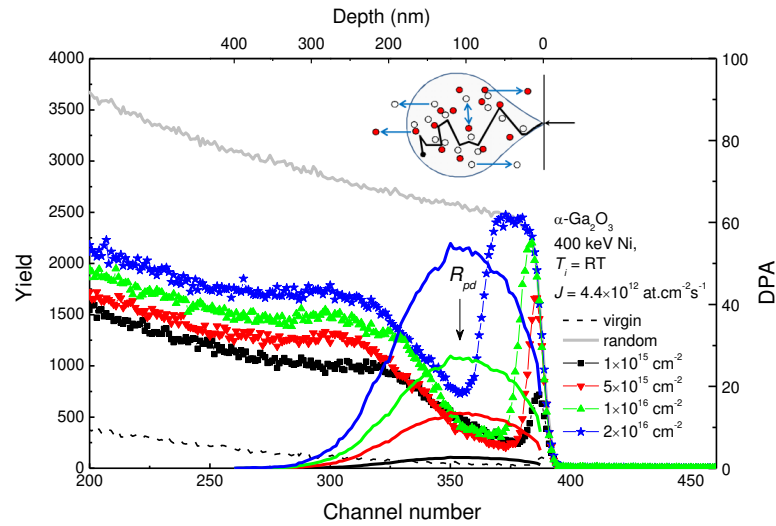


Fig. 1 Ga-parts of the RBS/C spectra of α -Ga₂O₃ implanted at room temperature with 400 keV ⁵⁸Ni⁺ ions to different ion doses keeping the same dose-rate (4.4×10^{12} at. cm⁻² s⁻¹) as indicated in the legend. The random and virgin (unimplanted) spectra are shown for comparison. The defect generation profiles in DPA (right-hand scale), as predicted with SRIM code simulations, are shown by the lines in correlation with Ga depth scale for the all the doses used, where the maximum of nuclear energy loss profile (R_{pd}) is indicated by the arrow. The inset shows schematics of the individual collision cascade generated by impinging ion (see the text for details).

This is the author's peer reviewed, accepted manuscript. However, the online version of record will be different from this version once it has been copyedited and typeset.

PLEASE CITE THIS ARTICLE AS DOI: 10.1063/1.50149870

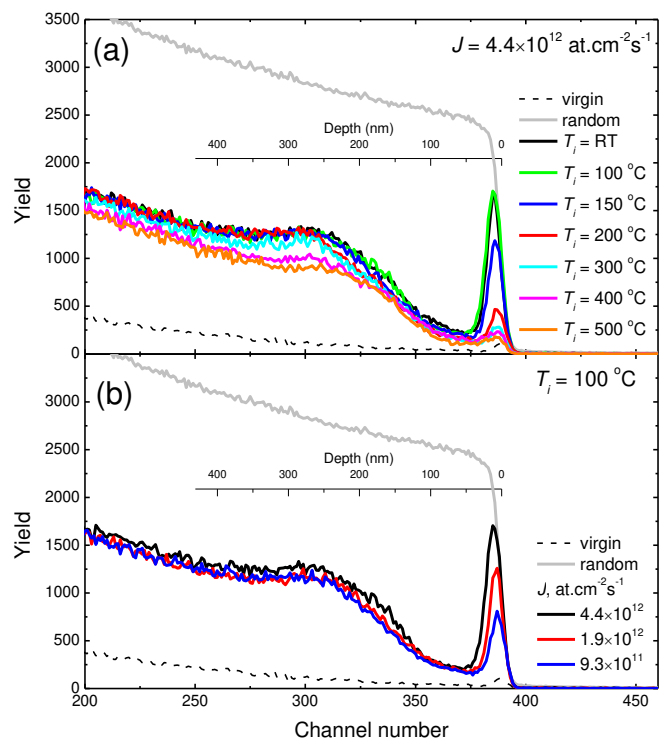


Fig. 2 Ga-parts of the RBS/C spectra of α -Ga₂O₃ implanted with 400 keV ⁵⁸Ni⁺ ions to the ion dose of $5 \times 10^{15} \text{ cm}^{-2}$ (a) at different temperatures keeping the same ion flux ($4.4 \times 10^{12} \text{ at. cm}^{-2} \text{ s}^{-1}$) and (b) at 100°C with the different fluxes as indicated in the legends. The random and virgin (unimplanted) spectra are shown for comparison.

This is the author's peer reviewed, accepted manuscript. However, the online version of record will be different from this version once it has been copyedited and typeset.

PLEASE CITE THIS ARTICLE AS DOI: 10.1063/1.50149870

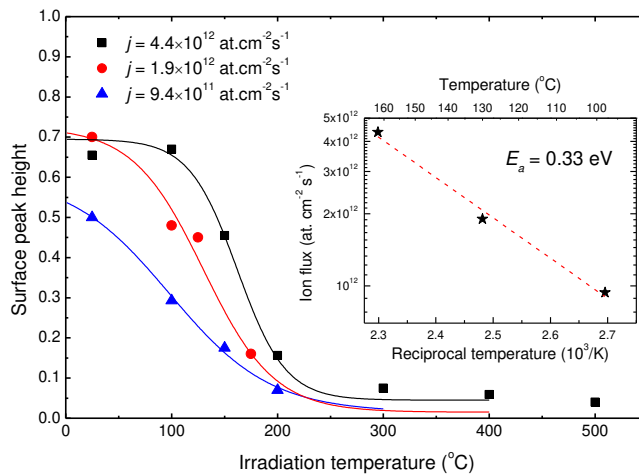
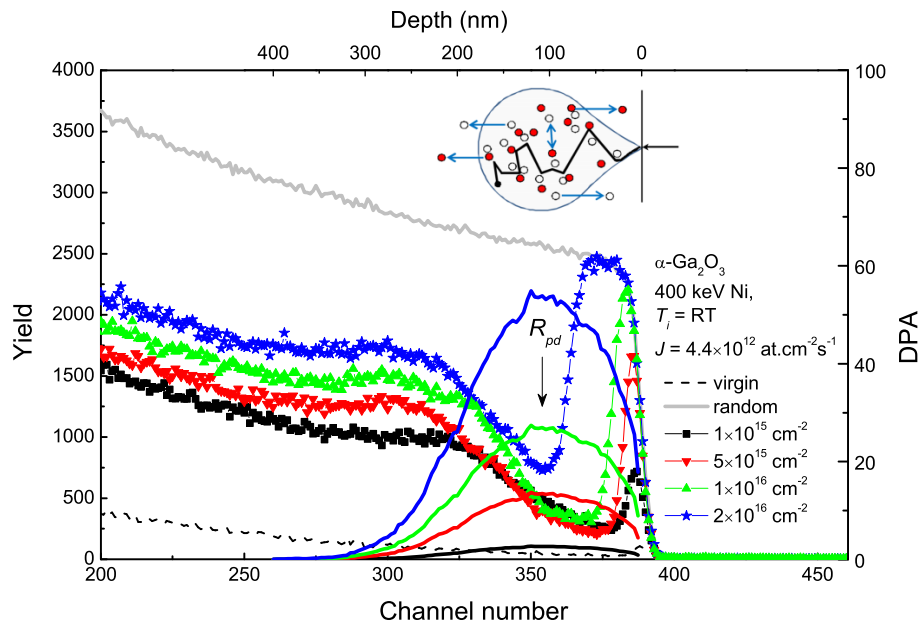


Fig. 3 Maximum relative surface disorder in α -Ga₂O₃ implanted with 400 keV Ni ions to $5 \times 10^{15} \text{ cm}^{-2}$ (as deduced from the RBS/C spectra) as a function of the irradiation temperature for different fluxes as indicated in the legend. The inset shows the Arrhenius plot for the ion flux vs the critical transition temperature as extracted from the fitting to the experimental data.

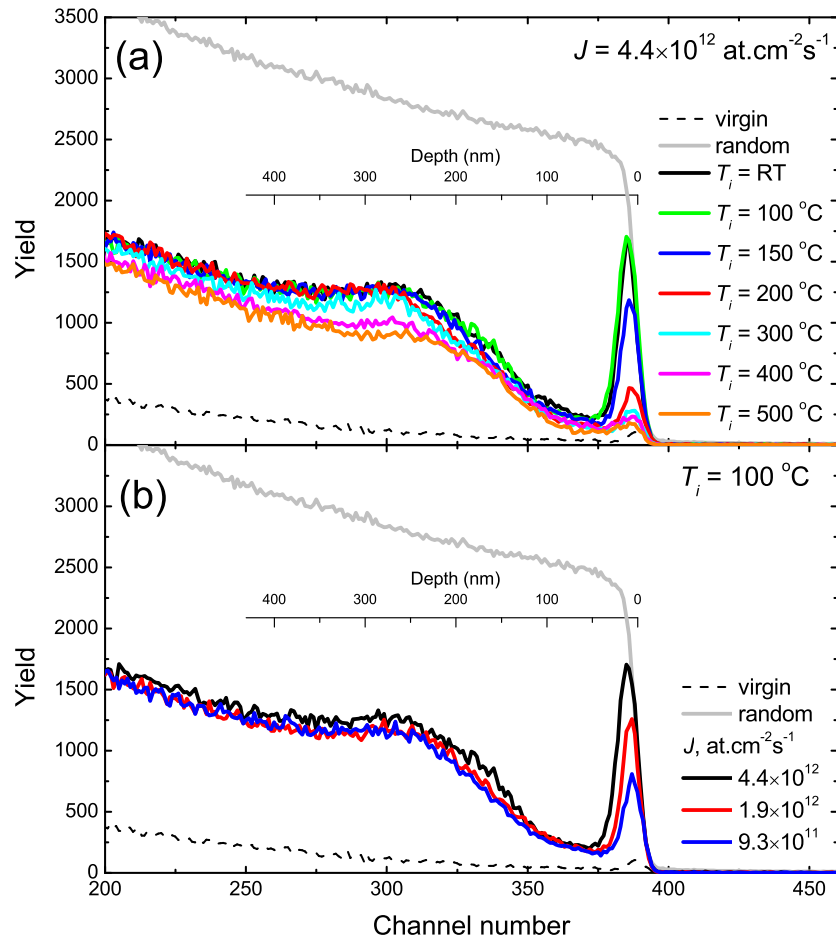
This is the author's peer reviewed, accepted manuscript. However, the online version of record will be different from this version once it has been copyedited and typeset.

PLEASE CITE THIS ARTICLE AS DOI: 10.1063/1.50149870



This is the author's peer reviewed, accepted manuscript. However, the online version of record will be different from this version once it has been copyedited and typeset.

PLEASE CITE THIS ARTICLE AS DOI: 10.1063/1.50149870



This is the author's peer reviewed, accepted manuscript. However, the online version of record will be different from this version once it has been copyedited and typeset.

PLEASE CITE THIS ARTICLE AS DOI: 10.1063/1.50149870

